

# Supplementary Information: Segregated Pt on Pd Nanotubes for Enhanced Oxygen Reduction Activity in Alkaline Electrolyte

*Samuel St. John*<sup>1</sup>; *Robert W. Atkinson, III*<sup>1</sup>; *Ondrej Dyck*<sup>1</sup>; *Cheng-Jun Sun*<sup>2</sup>; *Thomas A. Zawodzinski, Jr.*<sup>1,3</sup>; *Alexander B. Papandrew*<sup>1\*</sup>

1. Department of Chemical and Biomolecular Engineering, University of Tennessee, Knoxville,  
TN, USA.

2. X-ray Science Division, Argonne National Laboratory, Lemont, IL, USA.

3. Materials Science and Technology Division, Oak Ridge National Laboratory, Oak Ridge, TN,  
USA.

## AUTHOR INFORMATION

### **Corresponding Author**

\* Fax: (865) 974-7076; Tel: (865) 974-2421; E-mail: [apapandrew@utk.edu](mailto:apapandrew@utk.edu)

## EXPERIMENTAL DETAILS

**Nanotube Synthesis.** Palladium (PdNT), Platinum (PtNT), and Platinum-on-Palladium (PtPdNT) nanotubes were synthesized by a chemical vapor deposition within the pores of an anodic alumina membrane (Whatman Anodisc, 13 mm diameter, 200 nm pore size) by a technique reported previously.<sup>1</sup> A powder of palladium acetylacetonate (Alfa Aesar), or platinum acetylacetonate (Alfa Aesar), was confined beneath the alumina template and placed in a vacuum oven with 2.3 mL of deionized water. Air was evacuated from the oven by a rotary vane vacuum pump and replaced with dry N<sub>2</sub> several times before the pressure was reduced to 0.3 bar. The thermostat was set to a calibrated value of 170°C for Pd deposition, or 210°C for Pt deposition, and this temperature was maintained for 15 hours before the oven was flushed with dry N<sub>2</sub> and cooled to room temperature. For the bi-metallic nanotubes, precursors were deposited in sequential steps in separate vapor deposition experiments; Pt was deposited first, followed by Pd. The metal-bearing templates were thermally annealed to induce morphological evolution and to remove interstitial carbon absorbed during synthesis. After purging a quartz furnace tube for 30 minutes, the sample templates were heated for 1 hour at 250°C with flowing 4% H<sub>2</sub> (balance Ar) before they were allowed to cool passively to room temperature. The annealed sample templates were stirred in a 30% KOH solution at room temperature for 90 hours to dissolve the templates. Afterwards, the supernatant solution was decanted and replaced with de-ionized water until the nanotubes were suspended in a solution with neutral pH.

**Nanoparticle Synthesis.** Nanoparticle synthesis has been covered in detail before. Briefly, Pure Pd samples were synthesized via a single-step, chemical-vapor-phase deposition onto as-received Vulcan carbon XC-72R supports (~43%) using acetylacetonate precursors and similar methods to those previously published.<sup>19-21</sup> Solid Pd(acac)<sub>2</sub> precursor (Sigma-Aldrich) was

mechanically mixed in their appropriate stoichiometric ratios with as-received Vulcan XC-72R (Cabot) in a glass vial. The vial was placed in a vacuum oven along with a separate vial containing deionized water (Milli-Q, Millipore). The oven was sealed then purged with ultra-high-purity N<sub>2</sub>, evacuated to 0.30 bar, and heated to 240°C. During the thermal treatment, the liquid water vaporized, the organometallic precursors sublimed then decomposed, and metallic nanoparticles were deposited onto the support. After 15 h at 240°C, the oven was cooled to room temperature with a N<sub>2</sub> purge. The cooled samples were transferred to a quartz tube for reduction in a 4%-H<sub>2</sub>-in-Ar atmosphere at 240°C for 1 h.

### **Spectroscopy/Microscopy:**

*x-Ray Diffraction.* x-Ray diffraction (XRD) patterns were recorded with a Bruker Phaser D2 diffractometer using Ni-filtered Cu K $\alpha$  radiation ( $\lambda = 0.154184$  nm, 30 kV, 10 mA, 0.014° step, 1.0 s/step) in the Bragg-Brentano geometry fitted with a 0.6 mm antiscatter slit in the incident beam and a 2.5° Soller slit in the diffracted beam. The position and width of diffraction peaks were obtained by fitting to Voigt functions using IGOR Pro (Wavemetrics, Inc.).

*Transmission Electron Microscopy.* Nanotubes removed from the template were drop cast from water onto lacy carbon and dried under vacuum to collect high-resolution (HRTEM) images with a ZEISS Libra 200MC at an accelerating voltage of 200 kV.

*x-Ray Absorption Spectroscopy.* X-ray absorption spectroscopy (XAS) was conducted at beamline 20-BM at the Advanced Photon Source at Argonne National Laboratory (Argonne, IL, USA). Pre-edge correction, normalization, and post-edge subtraction via spline fitting were done in Athena.<sup>2</sup> The k<sup>2</sup>-weighted  $\chi(k)$  forward Fourier transform (FT) parameters were: k-weight, 0.5; window, Hanning; k-range, 22 – 16 Å<sup>-1</sup>. The k<sup>2</sup>-weighted  $\chi(R)$  backward FT parameters were: R-range, 1.8 – 3 Å; window, Hanning. Atomic first-shell scattering paths were simulated for

tetrahedral geometry (face-center, close-packed systems) for Pt and Pd using FEFF<sup>3</sup> and were fit simultaneously to the EXAFS data in Artemis to determine scattering path lengths.<sup>4</sup>

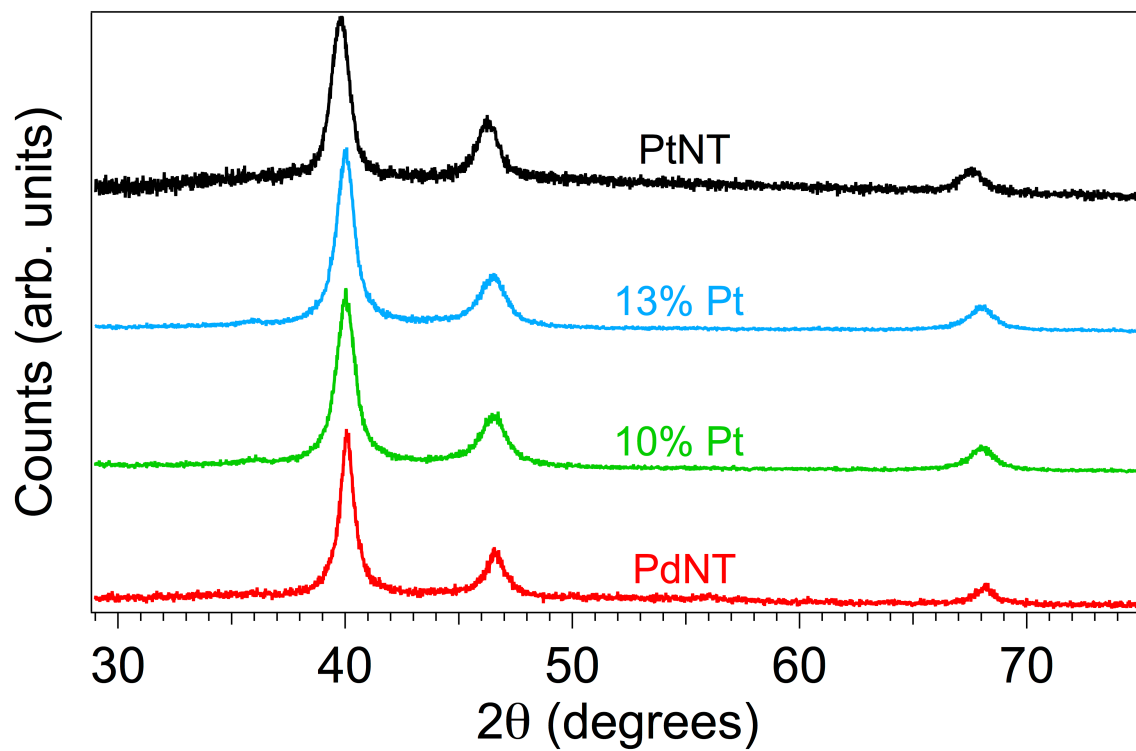
**Electrochemical Characterization:** Electrodes were made by depositing well-dispersed catalyst ( $12 \mu\text{g Pt-group metal/cm}^2_{\text{disk}}$ ) inks from a dilute solution ( $0.25 \mu\text{g of catalyst}/\mu\text{L}$ ) onto glassy-carbon electrodes ( $A = 0.196 \text{ cm}^2$ ) and dried slowly in a saturated atmosphere.<sup>5</sup> The nanotubes were easily dispersed by agitation with a pipette in water, while the carbon-supported catalysts were sonicated for three hours in an ice bath to form a homogenous suspension in a solution of 25% isopropanol with water.

Electrocatalysts were tested at room temperature in a standard three-electrode electrochemical cell (Pine Instruments) with a double-junction Ag/AgCl reference electrode (Pine Instruments) and Pt-wire counter electrode in  $\text{O}_2$ -saturated, 0.1M potassium hydroxide (semi-conductor grade, Sigma-Aldrich). Polarization curves were obtained at 10 mV/s over the range 0.05 – 1.1 V vs. RHE using a Bio-Logic VMP3 potentiostat. Potentiostatic electrochemical impedance spectroscopy (EIS) spectra were recorded from 200 kHz to 1 Hz at 0.6 V vs. RHE with a 10 mV sine perturbation amplitude under mass transport limited conditions and 1 atm  $\text{O}_2$ . The high-frequency intercept of the EIS spectrum was used to eliminate the ohmic resistance of the electrochemical cell from the polarization curves.

Electrochemical active surface areas (ECSAs) were obtained using Cu-stripping techniques on electrodes with  $\sim 25 \mu\text{g Pt-group metal/cm}^2$ .<sup>6</sup> The Cu-stripping polarization curves were integrated vs. the Cu-free catalyst baseline and divided by the sweep rate to obtain the total charge passed during Cu-stripping. ECSA was then obtained by dividing the integrated charge with the charge density of  $420 \mu\text{C/cm}^2_{\text{metal}}$ .<sup>6,7</sup>

Specific- and mass-normalized activities were obtained by dividing the resistance-corrected oxygen reduction current at 0.9 V vs. RHE by the real surface area or mass of the catalyst, respectively.

## RESULTS

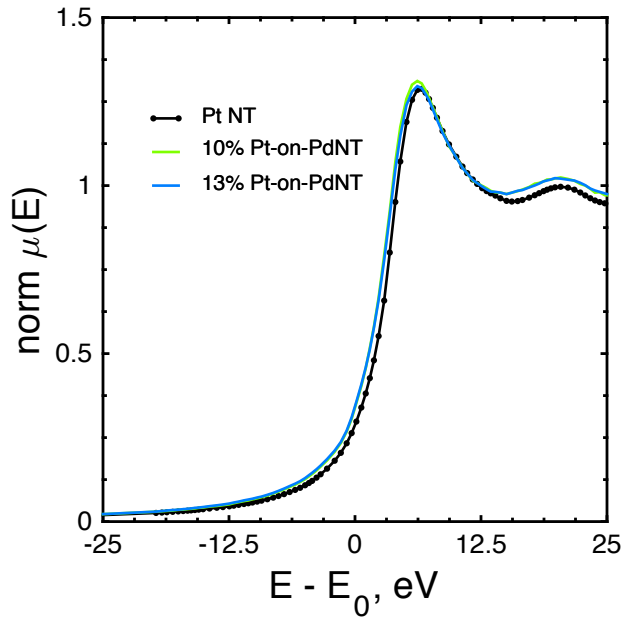


**SI Fig. 1:** Cu K $\alpha$  X-ray diffraction patterns for the PtNTs, PdNTs, and PtPdNTs collected after annealing in 4% H<sub>2</sub> at 250°C for 1 hour. Diffraction patterns illustrate the FCC composition of all of the catalysts with small shifts of the primary (111) diffraction peak for the bi-metallic nanotubes from either monometallic composition. The results of a Vegard's Law analysis indicate a degree of alloying of approximately 20% for the bi-metallic nanotubes suggestive of interfacial mixing between the Pt and Pd phases.

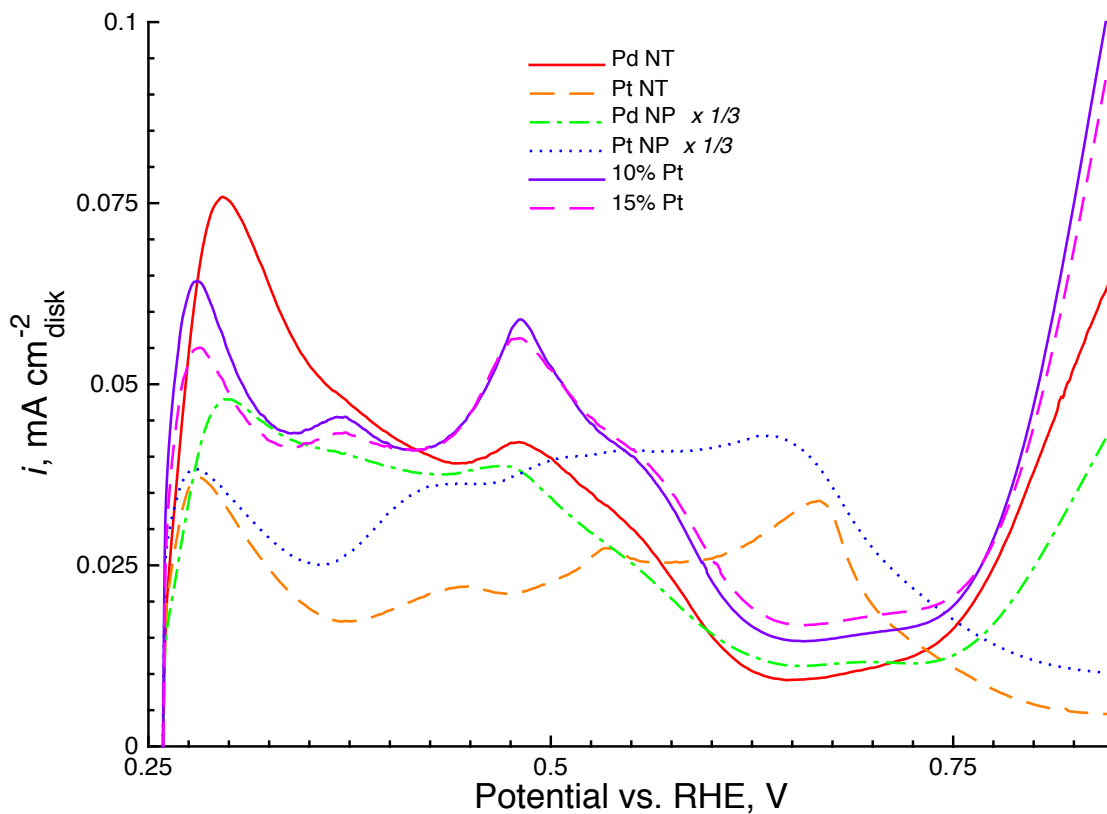
**SI Table 1:** Table of EXAFS fitted parameters for the investigated electrocatalysts.

Catalyst	Scattering		EXAFS Parameters for the indicated first-shell scattering path			
	Path*	Edge	$R$ (Å)	$\sigma^2$ (Å <sup>2</sup> )	$\Delta E_0$ (eV)	N
Pt foil	Pt-Pt	L <sub>3</sub>	2.759 ± 0.003	0.0046 ± 0.0002	5.013 ± 0.729	9.42 ± 0.62
Pd foil	Pd-Pd	K	2.734 ± 0.002	0.0053 ± 0.0003	1.862 ± 0.0423	9.40 ± 0.50
10% Pt	Pd-Pd	K	2.736 ± 0.003	0.0053	-2.206 ± 0.280	6.34 ± 0.11
10% Pt	Pt-Pt	L <sub>3</sub>	2.752 ± 0.012	0.0053	5.371 ± 2.765	7.83 ± 1.23
	Pt-Pd	L <sub>3</sub>	2.733 ± 0.033			1.91 ± 0.77
15% Pt	Pd-Pd	K	2.735 ± 0.010	0.0053	-2.177 ± 0.331	5.80 ± 0.18
15% Pt	Pt-Pt	L <sub>3</sub>	2.753 ± 0.013	0.0053	6.177 ± 1.150	6.52 ± 0.54
	Pt-Pd	L <sub>3</sub>	2.740 ± 0.019			2.24 ± 0.40

\* Scattering Path from Absorber (first atom given) to Scatterer (second atom given).

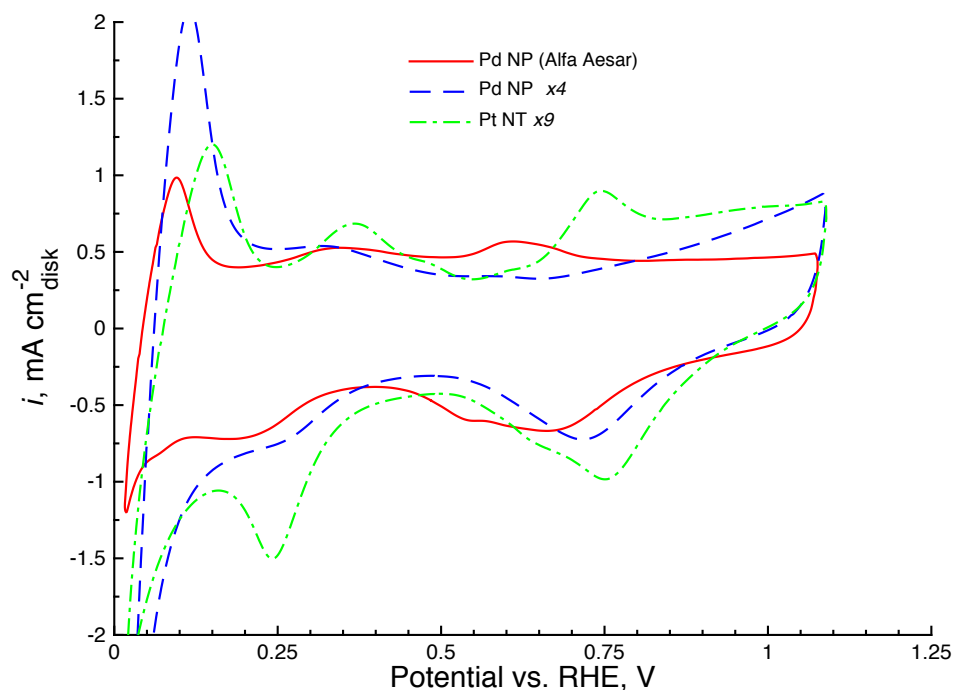


**SI Fig. 2:** Normalized XANES patterns for the monometallic PtNT and the two bi-metallic PtPdNTs at the Pt L<sub>3</sub> edge. There is a small shift of the step edge to lower values for the PtPdNTs suggestive of electron transfer from the supporting Pd nanotube to the surface-segregated Pt overlayer. The behavior is consistent with density-functional calculations for Pt overlayers on Pd, as well as the experimental charging currents collected in N<sub>2</sub>-saturated 0.1 M KOH. See the main text for a discussion of the results.

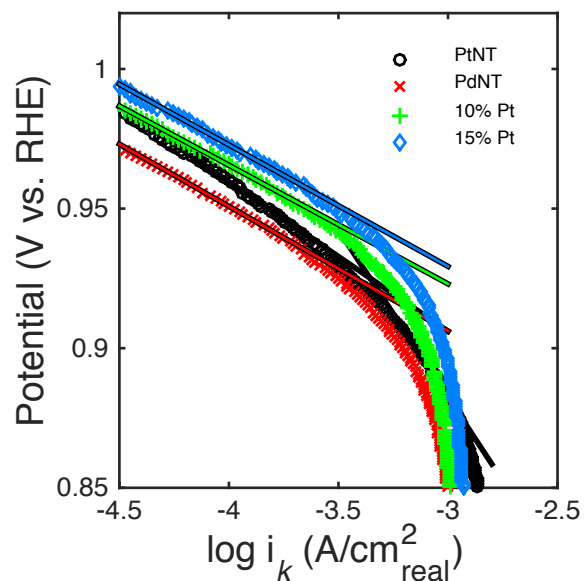


**SI Fig. 3:** Electrochemical data in static,  $N_2$ -saturated, 0.1M  $H_2SO_4$  with 2.5 mM  $CuSO_4$  collected at 10 mV/s for positive-going scans. The charging currents for the nanoparticles have been reduced using the factor indicated to more clearly illustrate the respective behavior of samples where there is a variation in the mass-normalized surface area. Currents were obtained by potentiostatically holding the electrode at  $\sim 0.25$  V vs. RHE for 5 minutes prior to sweeping the electrode.





**SI Fig. 4:** Electrochemical data in static,  $N_2$ -saturated, 0.1M KOH obtained at 10 mV/s. The charging currents for the Pd catalysts synthesized here have been multiplied by the indicated factor to more clearly illustrate differences because of differences in the contribution of carbon (for the Pd NPs) or from the lower surface area (Pd NTs). The Pd NPs from Alfa Aesar demonstrate the most oxophilic surface of the three Pd catalysts as evidenced by the leftward shift of the surface oxide reduction peak (negative peak) ca. 0.6 V vs. RHE. The charging current from the Pd NTs is characteristic of a bulk Pd surface and is the least oxophilic of the catalysts here. Such differences in oxophilicity impact the surface-area-normalized activity in a straightforward way. However, the size is apparently optimized for the size and site distribution obtained with the Pd NPs synthesized here.



**SI Fig. 5:** Tafel slope analysis for ORR in  $O_2$ -saturated, 0.1M KOH obtained at 10 mV/s and 1600 rpm for the nanotube samples as indicated in the figure. The lines are least-squares fits to the data at low current density/low overpotential. As is typical of polycrystalline catalysts, there is a smooth transition to an ill-defined Tafel slope at high current density/high overpotential. At low current density, the Tafel slopes are given in the main text and are in the range  $-40$  to  $-60$  mV/dec. At high current density, the  $-120$  mV/dec. slope is seen in the polycrystalline PtNT catalyst.

## REFERENCES

- (1) Papandrew, A. B.; Atkinson, R. W.; Goenaga, G. A.; Kocha, S. S.; Zack, J. W.; Pivovar, B. S.; Zawodzinski, T. A. Oxygen Reduction Activity of Vapor-Grown Platinum Nanotubes. *J. Electrochem. Soc.* **2013**, *160*, F848–F852.
- (2) Ravel, B. *EXAFS Analysis with FEFF and FEFFIT*; University of Washington, 2001; Vol. 2.
- (3) Rehr, J. J.; Kas, J. J.; Vila, F. D.; Prange, M. P.; Jorissen, K. Parameter-Free Calculations of X-Ray Spectra with FEFF9. *Phys. Chem. Chem. Phys.* **2010**, *12*, 5503–5513.
- (4) Ravel, B. *Crystallography for the X-Ray Absorption Spectroscopist*; University of Chicago, 2002.
- (5) Garsany, Y.; Baturina, O. A.; Swider-Lyons, K. E.; Kocha, S. S. Experimental Methods for Quantifying the Activity of Platinum Electrocatalysts for the Oxygen Reduction Reaction. *Anal. Chem.* **2010**, *82*, 6321–6328.
- (6) Shao, M.; Odell, J. H.; Choi, S.-I.; Xia, Y. Electrochemical Surface Area Measurements of Platinum- and Palladium-Based Nanoparticles. *Electrochem. commun.* **2013**, *31*, 46–48.
- (7) Shao, M.; Yu, T.; Odell, J. H.; Jin, M.; Xia, Y. Structural Dependence of Oxygen Reduction Reaction on Palladium Nanocrystals. *Chem. Commun.* **2011**.